Induced delocalization by correlation and interaction in the one-dimensional Anderson model

Conrad Albrecht* and Sandro Wimberger

Institut für Theoretische Physik, Universität Heidelberg, Philosophenweg 19, DE-69120 Heidelberg, Germany

(Received 18 March 2011; revised manuscript received 14 November 2011; published 9 January 2012)

We consider long-range correlated disorder and mutual interacting particles according to a dipole-dipole coupling as modifications to the one-dimensional Anderson model. Technically, we rely on the numerical exact diagonalization of the system's Hamilitonian. From the perspective of different localization measures, we confirm and extend the picture of the emergence of delocalized states with increasing correlations. Besides these studies, a definition for multiparticle localization is proposed. In the case of two interacting bosons, we observe a sensitivity of localization with respect to the range of the particle-particle interaction and insensitivity to the coupling's sign, which should stimulate new theoretical approaches and experimental investigations with, e.g., dipolar cold quantum gases.

DOI: 10.1103/PhysRevB.85.045107 PACS number(s): 61.43.−j, 03.75.Lm, 72.15.Rn

I. INTRODUCTION

When P. W. Anderson introduced a simple quantum model to represent a disordered lattice,[1] it turned out that the contained physics is surprisingly complex, i.e., there exists the phenomenon of Anderson localization, which is related to an exponential decay of the quantum mechanical probability distribution. A specific subclass of Hamiltonians Anderson studied reads

$$H_s = \sum_{i=1}^{L} \epsilon_i c_i^+ c_i + J \sum_{i=1}^{L-1} c_i^+ c_{i+1} + \text{H.c.}, \tag{1}$$

which represents a single particle in a one-dimensional chain of L sites with random onsite potential ϵ_i and kinetic (hopping) energy J. We assume the formalism of second quantization where the operator $c_i^{(+)}$ annihilates/creates a boson at site i, and hence we refer to Eq. (1) as the disordered Bose-Hubbard model without mutual interaction. One can either derive H_s from the tight-binding approximation of a continuous model[2] of noninteracting particles in an external potential or one takes it *ab initio* as a discrete model.

Based on the renormalization group flow idea (as usual in condensed matter physics, the flow is parametrized by the system size) one can argue that the conductance of a disordered solid may vanish for sufficient large systems.[3] In particular, the one-dimensional disordered system, Eq. (1), becomes an insulator in the limit $L \to \infty$.

An explicit argument for localization of all states $|E\rangle$ satisfying $H_s |E\rangle = E |E\rangle$ can be established by exploiting the transfer matrix method[4] and a theorem due to Fürstenberg.[5] On the other hand, there is Bloch's theorem,[6] which induces periodic, i.e. delocalized states for a periodic lattice potential ϵ_i. Hence the random nature of the potential must be obviously the key feature that leads to localization: a criterion based on the differentiability of the disorder potential ϵ_i was recently studied to understand the degree of randomness necessary for delocalization.[7]

In order to investigate the impact of correlation on localization, we introduce a specific disorder model that extrapolates from a pure random sequence $\epsilon_1, \epsilon_2, \ldots, \epsilon_L$ to a periodic, and thus correlated, structure in Sec. II. It was first used by Moura and Lyra[8] and similar investigations followed.[9,10] In a first step, we will review the model on the basis of three different localization measures. Furthermore, we utilize one of those quantities to establish the phase diagram—namely, the dependence of localization with respect to disorder strength and the amount of correlation among the ϵ_i. While a previous study by Shima *et al.*[11] focused on the properties of states in the band center, our measure in use accounts for the global aspect, i.e., it incorporates properties of the entire spectrum.

The potential interest in the sensitivity of Anderson localization on correlated disorder arose due to recent experiments with Bose-Einstein condensates (BECs) where the direct observation of the atomic density distribution provides access to the quantum-mechanical probability distribution.[12,13] Besides correlation, the impact of interaction is an issue one is naturally faced with when studying localization in BECs. Anderson already mentioned the importance of particle interaction[14] on localization and worked out theoretical investigations in collaboration with L. Fleishman.[15] Over the years, various aspects and features of interacting particles in a random potential have been figured out, but the problem remains a challenging topic for present research since results from different approaches do not always coincide. Just recently, the phase diagram of the three-dimensional disordered Bose-Hubbard model was established.[16]

In our discussion on interacting particles in the presence of a disordered onsite potential (see Sec. III), we first want to focus on a suitable definition of multiparticle localization and then turn to the extension of Eq. (1), namely,

$$H_{\text{mp}} = H_s + \sum_{i,j=1}^{L} U_{ij} c_i^+ c_j^+ c_i c_j, \tag{2}$$

with a two-body interaction potential U_{ij}. We model interaction according to a magnetic dipole-dipole coupling obtained in BEC experiments with dipolar gases,[17,18] which is beyond the standard treatment of the onsite interaction term $U_0 \sum_i \hat{n}_i(\hat{n}_i - 1)$ with $\hat{n}_i \equiv c_i^+ c_i$ present in the disordered Bose-Hubbard model. By explicitly diagonalizing H_{mp} for two interacting bosons, we explore the relevance of interaction, for localization, and discuss an interesting symmetry involving the sign of the interaction potential U_{ij}.

II. CORRELATED DISORDER

To model correlated disorder, we use the following prescription for the onsite potential values ϵ_i in Eq. (1):

$$\epsilon_i = \sum_{k=1}^{N/2} \left[\frac{2\pi k}{N}\right]^{-\alpha/2} \cos\left(\frac{2\pi}{N} ki + \phi_k\right) \quad \begin{cases} \alpha \geqslant 0, \\ N \gg L, \end{cases} \tag{3}$$

where $i = 1, \ldots, L$. Here, α denotes the correlation parameter, $\phi_k \in [0, 2\pi)$ are $N/2$ uniformly distributed random phases and N is a natural number that should be much larger than the number of lattice sites[19] L. Roughly speaking, the ϵ_i represent the discrete Fourier transform of $k^{-\alpha}$, i.e. they model an algebraic decaying power spectrum.[20] One is therefore used to refer to the ϵ_i as long-range correlated and, indeed, if we turn back to the continuum limit, we can argue that the ϵ_i are correlated according to an algebraic decay for $\alpha \in (0,1)$. The case $\alpha = 0$ corresponds to almost uncorrelated disorder, which is close to the perfect disorder Anderson assumed in his model. More details on properties of the ϵ_i from Eq. (3) are provided in Appendix.

A. Localization measures

In order to detect the localization-delocalization transition, we introduce three different measures: (a) the normalized standard deviation[21] (NSD), (b) the inverse participation ratio[22] (IPR), and (c) the nearest neighbor distribution[23] (NND).

While the NSD and the IPR are derived from the spatial/site probability distribution

$$\psi_E^2(i) \equiv |\langle i|E\rangle|^2 \quad \text{with} \quad H_s|E\rangle = E|E\rangle \quad \text{and} \quad |i\rangle \equiv c_i^+|0\rangle, \tag{4}$$

where $c_i\,|0\rangle = 0$, the NND depends on the spectral values E only. Given a chain of L sites, we calculate

$$\mathrm{NSD}(E) \equiv \frac{\langle i^2\rangle - \langle i\rangle^2}{(L^2-1)/12}, \tag{5}$$

where $\langle . \rangle \equiv \langle E\,|.|\,E\rangle$ denotes the expectation value, and hence the NSD derives the spatial variance of the lattice site index i for some $|E\rangle$ with respect to the state whose probability distribution is uniform on the lattice.

In the case of the IPR, one quantifies the inverse number of sites where $\psi_E^2(i)$ significantly differs from zero. Since $\langle E|E\rangle = \sum_{i=1}^{L} \psi_E^2(i) = 1$, we state that

$$\mathrm{IPR}(E) \equiv \sum_{i=1}^{L} \left[\psi_E^2(i)\right]^2 \sim \frac{1}{\tilde{L}}, \tag{6}$$

with $\tilde{L}$ defined as the number of sites that are occupied by $|E\rangle$. Indeed, we can convince ourselves that IPR ~ 1 and IPR $\sim L^{-1} \xrightarrow{L\to\infty} 0$ for localized and delocalized states, respectively.

In contrast, the NND considers the spectral properties of H_s. More precisely, we evaluate fluctuations of level spacings around a local mean $\bar{s}_n$ by computing

$$s_n \equiv (E_{n+1} - E_n)/\bar{s}_n \quad \text{with} \quad \bar{s}_n \equiv \frac{E_{n+1+\frac{m}{2}} - E_{n-\frac{m}{2}}}{m+1}, \tag{7}$$

and deriving the distribution $P(s)$ of the nearest-neighbor spacings s_n. Here, we labeled the spectral values according to $E_1 \leqslant E_2 \leqslant \cdots \leqslant E_L$ and the division by $\bar{s}_n$ unfolds[4] the level spacings to relate different parts of the whole spectrum to each other. The procedure of unfolding is not unique[24] and $m = 2m'$ with $m' \in \mathbb{N}$ is left as a free parameter that defines the notion of local. We choose it such that $m \ll L$, on the one hand, and we include enough energy values for reasonable statistics on the other hand; in fact, we used $m \sim 20$ for $L \sim 10^3$.

The NND is not as obvious as the former measures.[25,26] Intuitively, the argument works as follows. Taking two different energy eigenstates $|E\rangle, |E'\rangle$ that do not significantly overlap in site space, we assume them to be almost orthogonal, i.e., they are in some sense independent from each other and nothing prevents the corresponding energy values to be arbitrary close, $s \to 0$. But if the overlap increases (extended states), the levels start to repel, $E \neq E'$.[27] Quantities that are statistically independent exhibit a Poissonian distribution and thus the corresponding NND should be[28] $P(s) \sim e^{-s}$. In contrast, $P(s=0) = 0$ is reasonable to expect for delocalized states.

B. Numerical results

Turning back to Eq. (1) we rescale H_s by J, i.e., $H_s \to J^{-1}H_s$, which does not alter the Hamiltonian's eigenstates but multiplies the spectral values E by a factor of J^{-1}. Since we restrict the ϵ_i to the finite interval $[-\frac{\Delta}{2}, \frac{\Delta}{2}]$, we introduce the parameter

$$\kappa \equiv \Delta/J \tag{8}$$

that indicates the strength of disorder. Thus we are faced with a two-dimensional set of system parameters (α,κ) and from the following as well as Appendix, it becomes clear that increasing α corresponds to increasing correlations up to long-range correlated disorder. Moreover, since the NSD and the IPR only depend on $|E\rangle$, we rescale and shift the spectrum such that the rescaled values $E \to e$ obey $-0.5 \leqslant e \leqslant 0.5$ when plotting these quantities resolved in energy.

To set the stage, we want to relate our numerical results to previously published ones. Since it is common practice to attempt localization by computing the Lyapunov exponent,[4] we establish an exponential fit to $|E\rangle$.[29] More precisely, our numerics picks out the maximum $\psi_E^2(i_0)$ and performs an exponential fit into the direction singled out by $\max(i_0, L - i_0)$. From $\psi_{E,fit}^2(i) \sim \exp(-\gamma\,|i - i_0|)$ we extract $\gamma(E)$ and define the localization length

$$\mathrm{LL}(E) \equiv \gamma^{-1}(E)/L. \tag{9}$$

The corresponding result for intermediate disorder $\kappa = 1$ is shown in Fig. 1 and it exhibits reasonable qualitative agreement with Ref. 8, Fig. 5; namely, delocalized states $\gamma^{-1} \sim L \to \mathrm{LL} \sim 1$ arise in a finite range around the band center $e = 0$ when the correlation within the disorder potential ϵ_i is increased. This interpretation also coincides with the plot presented in Ref. 9, Fig. 3, where localization was quantified by means of a measure based on the density of states

$$\mathrm{DOS}(E) \equiv \frac{dn}{dE}, \tag{10}$$

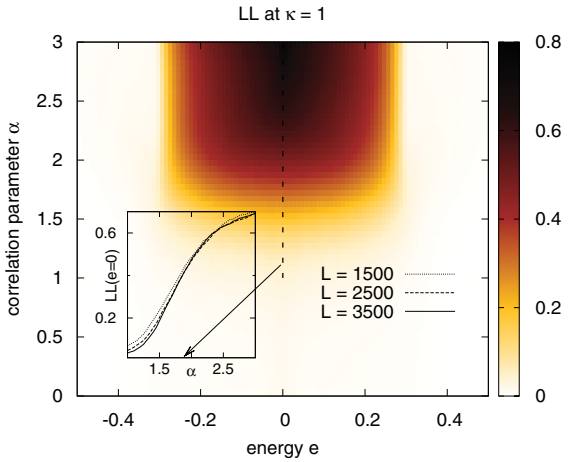

FIG. 1. (Color online) Energy-resolved plot of the localization length LL for different correlation parameter values α to compare our results from exact numerical diagonalization to investigations that use the transfer matrix method to obtain the Lyapunov exponent γ, cf. Ref. 8, Fig. 5. We used a system of $L = 3500$ sites and averaged over 50 disorder realizations. The inset transparent to the main panel in the background presents numerical data of LL(0) for different system sizes, which underpins the reported delocalization transition around $\alpha = 2$.

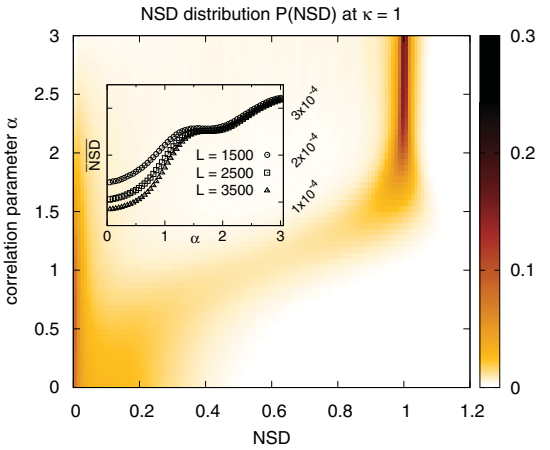

FIG. 2. (Color online) Plot of the distribution P(NSD) of the spatially normalized standard deviation, see Eq. (5), at intermediate disorder, $\kappa = 1$; it supports that localization→delocalization takes place rather smoothly than according to a sharp transition. As for Fig. 1, we used $L = 3500$ and the averaging was taken over 50 disorder realizations. The inset transparent to its background shows results for different system sizes and supports our crossover picture. A more detailed description is given in the main text.

which defines the number dn of energy eigenstates $|E\rangle$ in a given interval $[E, E + dE]$. In particular, $\int_{E_1}^{E_2} dE\mathrm{DOS}(E)$ is the number of states $|E\rangle$ with $E_1 \leqslant E \leqslant E_2$ and rescaling the DOS simultaneously with the spectrum $\{E\}$ is understood to fulfill the normalization condition $1 = \int dE\mathrm{DOS}(E)$.

Moreover, the work of Moura and Lyra mentioned above supports delocalization at $\alpha = 2$ for states at the band center. Therefore we depicted a cut of Fig. 1 at $e = 0$ (dashed line) in the relevant correlation parameter range $\alpha \in [1,3]$ and checked LL(0) according to a finite size analysis, inset of Fig. 1. Indeed, up to $\alpha \approx 2$, the LL(0) decreases with increasing system size L, while above this correlation parameter value it remains relatively constant. Assuming that this trend persists for even larger system sizes, the data support that $\alpha = 2$ marks a qualitative difference between systems with smaller and larger correlation, respectively. While the relative extent of the states with respect to the system size falls off for $0 \leqslant \alpha \lesssim 2$, it remains constant for $\alpha \gtrsim 2$ in the thermodynamic limit, $L \to \infty$ (extended states).

However, we would like to address the question where in terms of α does the localization-delocalization transition takes place from the perspective of the measures introduced in Sec. II A. Instead of a sharp transition at $\alpha = 2$, which is supported by Fig. 1 and publications mentioned above, we suggest a smooth crossover in $1 \lesssim \alpha \lesssim 2$. Investigating the distribution P(NSD) most obviously illustrates this statement and we present it in Fig. 2. Although the major fraction of localized states (NSD $\ll 1$) becomes delocalized at $\alpha \approx 2$, there is a finite fraction that splits apart the localized region $0 \leqslant \mathrm{NSD} \lesssim 0.2$ around $\alpha = 0.5$ and drifts toward the delocalized regime NSD ≈ 1 up to $\alpha \approx 2$. This observation remains stable in the numerically studied range of system sizes $L = 1000, \ldots, 3500$.

An explicit plot of the finite-size analysis performed with respect to our crossover picture is given by the inset of Fig. 2. Convoluting the NSD with the DOS, i.e.,

$$\overline{\mathrm{NSD}} \equiv \int dE\mathrm{NSD}(E)\mathrm{DOS}(E), \tag{11}$$

yields a single quantity to characterize the global localization property of the disorderd system at fixed correlation parameter α. In the spirit of the previously applied LL dependence on L, the inset of Fig. 2 provides the system size dependence of the averaged normalized standard deviation $\overline{\mathrm{NSD}}$; up to $\alpha \approx 1.5$, $\overline{\mathrm{NSD}}$ decreases with increasing system size L indicating that the Hamiltonian's eigenstates stay localized in the thermodynamic limit. Above $\alpha \approx 1.5$, the averaged standard deviation that is normalized to L remains unaltered for the accessed number of sites—a signature of delocalization from this global point of view. Remarkably, the numerical data of $\overline{\mathrm{NSD}}$ form a plateau in at least $1.5 \lesssim \alpha \lesssim 2$, before growing up in absolute value with increasing correlation, which is more evidence to the crossover picture we are in favor of.

Similarly, we investigate the IPR taking into account the DOS from Eq. (10). Since we are interested in the localization property of the whole system, it is necessary to account for the number of states with a certain localization measure value. Hence the IPR and the DOS are plotted simultaneously in Fig. 3 and the inset of the upper panel presents an averaged version of the inverse participation ratio in total analogy to Eq. (11) with NSD(E) replaced by IPR(E).

From a naive point of view, we could conclude that even for weak correlation, $\alpha \lesssim 0.5$, the system is delocalized, since there are only a few localized states near the band edges, $|e| = 0.5$, while the rest of the spectrum exhibits an IPR value corresponding to delocalization. Moreover, increasing correlation enhances localization up to $\alpha \approx 1$, which seems unexpected. But if we include the DOS (lower panel of Fig. 3), the picture drawn before reveals: we realize that almost

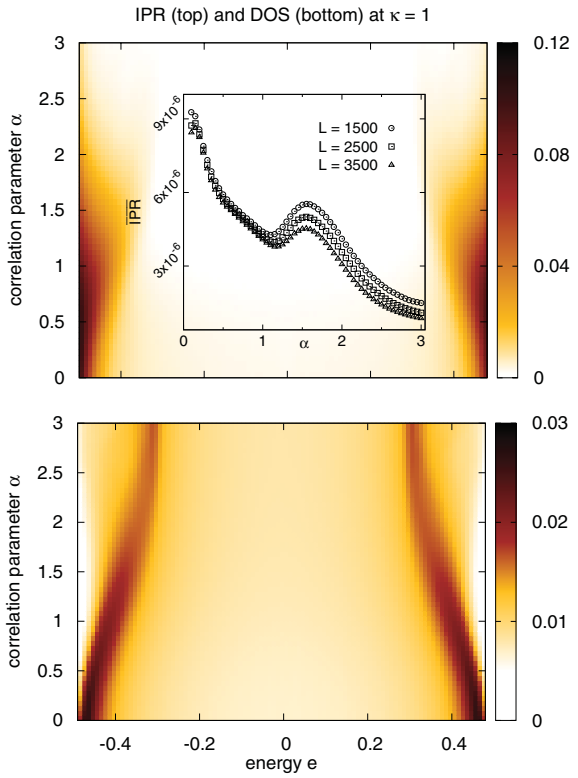

FIG. 3. (Color online) Smooth localization-delocalization crossover from the perspective of the simultaneous analysis of the IPR and the DOS. Increasing correlation attracts the system's states from the band edges $|e| = 0.5$ to the band center $e = 0$ where delocalized states are present and thus the system becomes more and more delocalized. Finally, localized states almost completely vanish above $\alpha = 2$. The inset of the upper panel (transparent to the background again) establishes the finite-size analysis similar to the inset of Fig. 2.

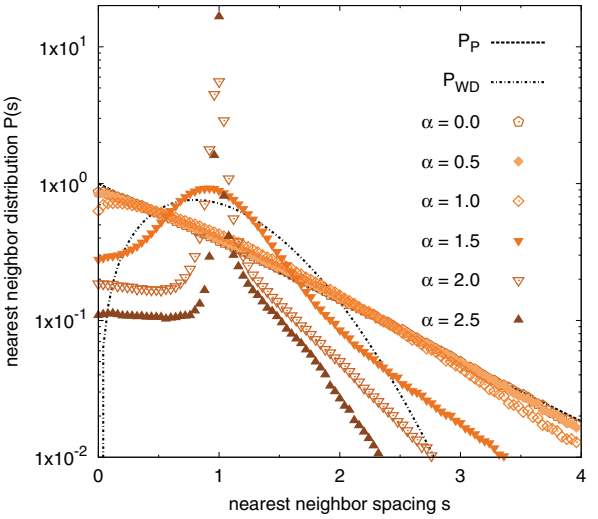

FIG. 4. (Color online) Semilogarithmic plot of the nearest-neighbor spacing distributions for several correlation parameter values α ($L = 3 \times 10^4, \kappa = 1$). The broken line compares them to the Poissonian distribution P_{P}, which we expect for localized states. As apparent, the distribution does not converge to P_{WD} of the Gaussian orthogonal ensemble[4] since for $\alpha \gg 1$ the onsite potential ϵ_i becomes periodic, local fluctuations among the E_i vanish and thus $P(s)$ has to be peaked around $s = 1$, $s_n = (E_{n+1} - E_n)/\bar{s}_n \approx 1, \alpha \gg 1$. A more detailed discussion is given in the main text.

all states have energies near to the band edges for $\alpha \lesssim 0.5$ and thus the system is localized. The crucial fact leading to the localization-delocalization crossover is that for increasing correlation, the band center attracts the states from the band edges to the regime where delocalized states are permanently present, $|e| \lesssim 0.3$. Localized states at the band edges follow that trend only up to $\alpha \approx 1$ and, for stronger correlation, they start to disappear until they are almost vanished at $\alpha \approx 2$. According to an argument presented in Appendix, it is reasonable to refer to disorder with $\alpha \geqslant 1$ as highly correlated and therefore it provides a hint to the suggestive importance of $\alpha = 1$ in our data.

Again, this observation is confirmed by a finite-size analysis as shown in the inset of the upper panel of Fig. 3. We note that the $\overline{\mathrm{IPR}}$ values stay quite unaltered for $\alpha \lesssim 1$ when L is increased. Since $\mathrm{IPR} \sim \tilde{L}^{-1} \sim L^{-1}$ corresponds to extended states, which tend to zero in the limit $L \to \infty$ (cf. Eq. (6)), the decreasing behavior of $\overline{\mathrm{IPR}}(L)$ for $\alpha \gtrsim 1$ suggests the existence of delocalized states. The bump in the crossover interval $\alpha \in [1,2]$ may represent a finite-size effect that eventually vanishes in the thermodynamic limit.

Finally, we would like to take a closer look at the smooth crossover from the perspective of the energy spectrum. Therefore we investigate the NND from Sec. II A, which also prepares the relevant measure we will use to quantify the (κ,α) dependence of localization. Plots of the NND for different correlation parameters α are presented in Fig. 4. For small α, the result is near to the Poissonian distribution e^{-s}. Deviations from the theoretical prediction are due to the finite system size L and the fact that $\alpha = 0$ does not exactly correspond to uncorrelated but weakly correlated disorder, see Appendix. We further observe that the data points for $\alpha = 0$ and 0.5 almost coincide, but when increasing α above 0.5, the distribution starts to deviate more significantly from e^{-s} to become peaked around $s = 1$. Returning to Eq. (3), we note that for $\alpha \gg 1$ the summation over the discrete momenta k picks up less cosine modes, which leads to a periodic onsite potential in the limit $\alpha \to \infty$. Hence the spectrum of H_s becomes more regular for increasing α and local fluctuations eventually vanish for sufficiently strong correlation due to Bloch's theorem. From the definition of the unfolded level spacings s_n, see Eq. (7), we conclude that all s values should be centered around 1 due to the normalization by the local mean $\bar{s}_n$.

At this stage, it is advisable to discuss the Wigner surmise P_{WD}—a specific NND connected to random matrix theory[4]—in the context of localization, especially, in our specific model system under consideration. In the literature,[30–32] it seems to be common practice to associate

$$P_{\mathrm{P}}(s) \equiv \exp(-s) \tag{12}$$

with localized states and signatures of level repulsion $P(s \ll 1) \ll 1$ in the NND with extended ones after having unfolded the spectrum of the corresponding disordered system. In the case of a time reversal symmetric quantum chaotic

system—represented by real, symmetric random matrices—the NND adopts the Wigner surmise

$$P_{\mathrm{WD}}(s) \equiv \frac{\pi}{2} s \exp\left(-\frac{\pi}{4} s^2\right) \tag{13}$$

in the thermodynamic limit, cf. Ref. 4 as well as references therein.

As we sketched it in Sec. II A, it is quite plausible to assume the first correspondence to be valid. Indeed, the matrix representation of H_s in the site basis $\{|i\rangle\}$ becomes tridiagonal, i.e.,

$$H_{s,ij} \equiv \langle i\,|H_s|\,j\rangle \tag{14}$$

vanishes except for its diagonal elements $H_{s,ii} = \epsilon_i$ and the first off-diagonal entries $H_{s,ii+1} = H_{s,i+1i} = J$ when open boundary conditions, cf. Appendix, are imposed. In the limit where the uncorrelated disorder strongly dominates the kinetic energy, i.e. $\Delta \gg J$, the single-particle Hamiltonian becomes approximately diagonal to zeroth order in $\frac{J}{\Delta}$ and the solution to the Schrödinger equation reads $|E_i\rangle \approx |i\rangle$ with $E_i \approx \epsilon_i$. Hence the almost purely random/uncorrelated sequence of eigenvalues E_i should obey a Poissonian distribution in the NND.

On the other hand, the Hermitian operator $H_{s,ij}$ is composed from real valued entries including random elements that correspond to realizations of the correlated disorder ϵ_i, where $i = 1, \ldots, L$. At first glance, it might be therefore reasonable that the distribution P_{WD}, associated with the Gaussian orthorgonal ensemble[33] (GOE), may arise for $\alpha \neq 0$. In fact, one is able to explicitly construct an ensemble of random, tridiagonal, and symmetric matrices: the β-Hermite ensemble with $\beta = 1$ that obeys the same joint eigenvalue probability density $p(E_1, E_2, \ldots, E_L)$ as in the GOE case.[34] Furthermore, numerical simulations confirmed the Wigner surmise being appropriate to characterize the NND in the thermodynamic limit.[35] Moreover, investigations like, e.g., Ref. 30, report the emergence of P_{WD} in the metallic phase of a three-dimensional disordered electron gas, and Ref. 36 (see also references therein) considers the so-called two-body random interaction model where a sufficiently strong interaction magnitude takes the NND to P_{WD}. Systematic numerical studies of those sparse random matrix Hamiltonians also yielded evidence that the statistics of s is suitably described by the Wigner surmise.[37]

But as explicitly illustrated in Fig. 4, we do not observe P_{WD} in our specific model system. More precisely, the NND significantly deviates from the Wigner surmise in the limit $\alpha \to \infty$; cf. our motivation of a peaked structure for the NND in this limit above. The message we would like to carve out at this point is the following: although the literature provides well established examples of disordered systems, which support P_{WD} when deriving the NND, one should not expect it to be valid from the outset. In particular, our studies provide a counterexample to it. Therefore, the approach to detect the transition from localization to delocalization by some critical distribution P_c that is designed to interpolate between P_{P} and P_{WD} is not well justified in our case and we will discuss this issue in detail in the following paragraphs, cf. Eq. (18), Figs. 5 and 6.

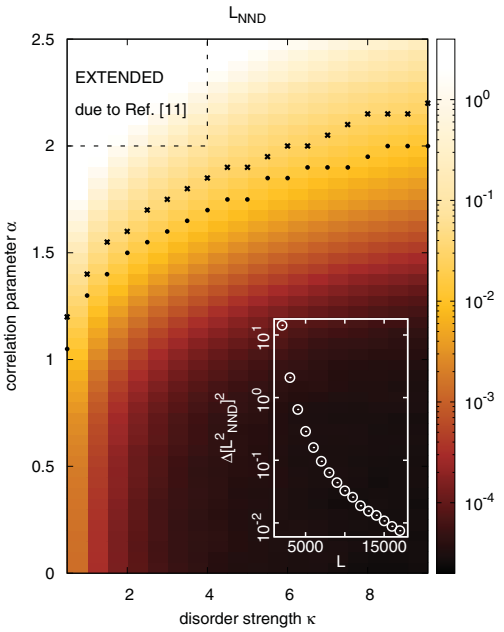

FIG. 5. (Color online) (κ,α) dependence of localization in the one-dimensional Anderson model from the perspective of a measure based on the nearest-neighbor spacing distribution NND of the Hamiltonian's spectrum with $L = 3 \times 10^4$. The finite-size analysis with the measure $\Delta[L^2_{\mathrm{NND}}]^2$, defined in Eq. (17), is shown as a white inset. Furthermore, we included the region that corresponds to extended states according to the work of Shima *et al.*[11] who tackled the phase diagram by means of states in the band center $E = 0$ using the transfer matrix method. The symbols • mark the minimal deviation of the NND from P_{SP}, cf. Eq. (18), for fixed disorder strength κ and the symbols $\times$ indicate the same minima with respect to P_{WD}, Eq. (13).

One way to extract the localization-delocalization transition by means of a suitable P_c is performed in, e.g., Ref. 30. Usually, one investigates the quantity

$$\eta \equiv \frac{\int ds[P(s) - P_{\mathrm{WD}}(s)]}{\int ds[P_{\mathrm{P}}(s) - P_{\mathrm{WD}}(s)]} \tag{15}$$

based on the NND $P(s)$ where the integrals may be chosen on a suitable interval where one expects sensitivity of $P(s)$ on localization. According to our discussion from Sec. II A one may take $s \in [0, s_{\max}]$ with $s_{\max}$ smaller than the smallest root of $P_{\mathrm{WD}}(s) = P_{\mathrm{P}}(s)$. But since our one-dimensional disordered system in use does not converge to the Wigner surmise, it is rather vague to apply Eq. (15) in order to resolve the question on the impact of correlation on localization.

Nevertheless, the previous discussion invites us to introduce a similar measure for plotting the dependence of localization on the parameter space (α,κ), which will be the last purpose of this section on correlated disorder. We determine the deviation of $P(s)$ from P_{P} as a quantity for the degree of delocalization. Thus we define

$$L^2_{\mathrm{NND}}(\kappa,\alpha) \equiv s_{\max}^{-1} \int_0^{s_{\max}} ds[P(s,\kappa,\alpha) - P_{\mathrm{P}}(s)]^2, \tag{16}$$

where, in our case, $s_{\max}$ introduces the numerically necessary restriction to a finite range of s values and we use $L_{\mathrm{NND}} \equiv \sqrt{L^2_{\mathrm{NND}}}$ as a localization measure. Numerically, L_{NND} features

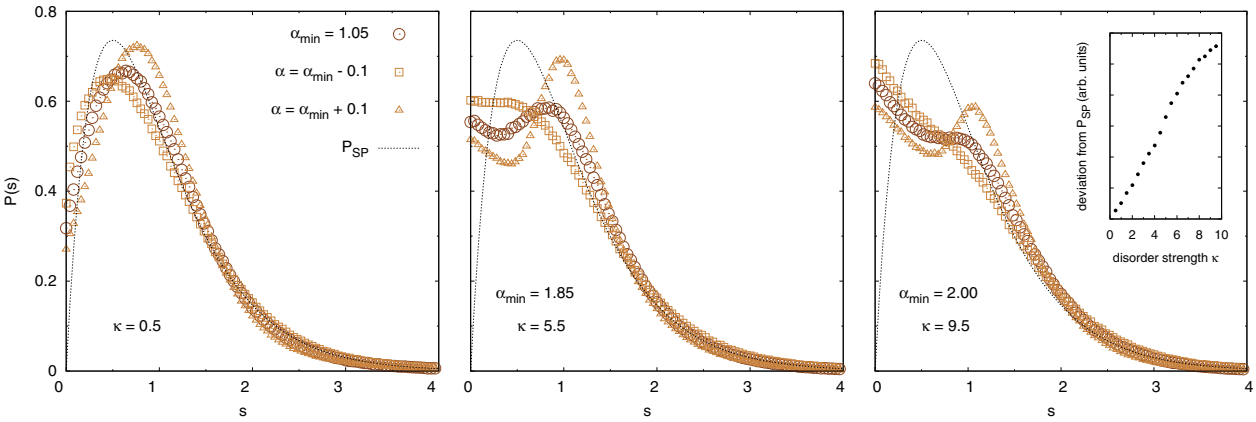

FIG. 6. (Color online) NNDs for different disorder strengths κ and $L = 3 \times 10^4$ illustrate that the semi-Poisson law P_{SP} as a hybrid between the Poisson distribution P_{P} and the Wigner surmise P_{WD} is not an appropriate critical distribution to indicate delocalization for our model under consideration. The NND $P(s)$ with α_{min}, denoted by symbols $\odot$, is singled out by its minimal deviation from P_{SP} for fixed κ as described in the main text, cf. also symbols $\bullet$ in Fig. 5. Plotting $P(s)$ with $\alpha_{\mathrm{min}} \pm 0.1$ underlines the two statements we emphasized: (a) decreasing values of the NND for $s \to 0$ (level repulsion) and (b) development of a peak of $P(s)$ around $s = 1$ for increasing correlation parameter α due to extended states (increase of $P(1)$). The inset in the right panel shows the absolute increase of the minimal deviation from P_{SP} when disorder becomes more dominating.

the striking advantage that it is sufficient to just compute the eigenvalues of the Hamilton matrix $H_{s,ij}$, and therefore we are able to reach larger system sizes L with our code.

As we know from the previous considerations on the localization-delocalization crossover for intermediate disorder $\kappa = 1$, cf. the first part of Sec. II B, correlation with $1 \leqslant \alpha \leqslant 2$ seems to be important for delocalization; varying α in $[0,2.5]$ will cover it. In the limit $\kappa \to 0$, i.e., vanishing disorder, it is obviously hardly possible to recover Anderson's result for infinitely extended systems and arbitrary small disorder, since we have to face the fact to be generally restricted to finite system sizes L and finite numerical precision. Therefore we investigate the domain $(\alpha,\kappa) \in [0,2.5] \times [0.5,10]$, which spans a wide range of disorder strengths κ for the interesting amount of correlation among the onsite disorder potential values ϵ_i. The corresponding result is shown in Fig. 5 with $L = 3 \times 10^4$ and the inset presents the finite-size analysis we performed. Let ΔL denote the fixed difference between two system sizes L and L' such that $L = L' + \Delta L$, and we define

$$\Delta\left[L^2_{\mathrm{NND}}\right]^2(L,\Delta L) \equiv |\mathcal{A}|^{-1} \int_{\mathcal{A}} d\kappa d\alpha \left[L^2_{\mathrm{NND}}(\kappa,\alpha,L) - L^2_{\mathrm{NND}}(\kappa,\alpha,L')\right]^2 \tag{17}$$

with $|\mathcal{A}| = |[0,2.5] \times [0.5,10]| = \Delta\kappa\,\Delta\alpha$ the area of integration. The white inset plots that quantity versus L having fixed $\Delta L = 1000$; it becomes clear that Fig. 5 exhibits a convergent trend for increasing L.

Before turning to a more detailed analysis of $L_{\mathrm{NND}}(\kappa,\alpha)$, let us come back to our comments on a critical distribution P_c. As stated before, we do not expect the NND to converge to P_{WD} in the limit $\alpha \to \infty$. In our case, it is not well justified to assume, e.g., the semi-Poisson law[31]

$$P_{\mathrm{SP}}(s) \equiv 4s \exp(-2s), \tag{18}$$

which resembles the linear increase of $P_{\mathrm{WD}}(s)$ for $s \ll 1$ and an exponential decay for $s \gg 1$, to be critical. Numerical evidence on our claim provides Fig. 5 where we plot both the minimal deviation of the NND from P_{SP}, symbols $\bullet$, and P_{WD}, symbols $\times$, for fixed disorder strength κ. The notion deviation is defined in total analogy to Eq. (16). In the case of the convergence of the NND to P_{WD}, we would expect the minima $\times$ to appear at the maximal α value simulated—independent from the disorder strength κ. But, as visible in Fig. 5, the NND passes by P_{WD} below $\alpha \approx 2.2$. Surprisingly, the deviation minima of the NND from P_{SP}, symbols $\bullet$, appear to lie in the crossover region $1 \leqslant \alpha \leqslant 2$ we emphasized during our previous numerical studies. Moreover, they follow the qualitative trend of our localization measure L_{NND}, which one may naively exploit to argue in favor of P_{SP} as a suitable critical distribution. But a closer look on the precise shape of the NND with minimal deviation from P_{SP} reveals significant differences from the semi-Poisson law that become even more obvious with increasing disorder strength κ. A corresponding plot is shown in Fig. 6. Therefore, we do not support the semi-Poisson law P_{SP} as a suitable critical distribution. In fact, it is designed as a hybrid between the two limiting cases of a Poisson distribution P_{P} and the Wigner surmise P_{WD}, which does not apply to extended states in our specific model.

However, there has been a similar investigation to our phase diagram in Ref. 11 and we would like to discuss some conclusions one may draw when comparing the two results now. Shima *et al.* report numerical studies that support the existence of extended states for $(\kappa,\alpha) \in [0,4] \times [2,5]$ (according to their notation κ translates to W and α to p) on basis of a quantity Λ similar to our LL evaluated at the band center $e = 0$, cf. their Fig. 6. We separated the corresponding region of extended states in Fig. 5 by a dashed line. There are two main differences we would like to point out with respect to our investigations of $L_{\mathrm{NND}}(\kappa,\alpha)$. First of all, the localization-delocalization crossover depends on the disorder strength, and second, L_{NND} varies over approximately two orders of

magnitude in $1 \lesssim \alpha \lesssim 2$ quite independently from the value κ. Therefore the evaluation of the NND underlines the picture of a smooth crossover between localization and delocalization drawn before. The qualitative result of delocalization for all κ values under consideration is in accordance with our line of reasoning that the disordered system has to eventually delocalize for $\alpha \to \infty$ due to Bloch's theorem. Therefore it would be interesting to push the numerical analysis of Shima *et al.* beyond their maximal correlation $\alpha \leftrightarrow p = 5$. However, assuming that the deviation of the results of Shima *et al.* and our investigations is not caused by some hidden technicality,[38] the discrepancy of our conclusions to Shima *et al.* may reveal two useful lessons: (1) it reminds us of the difficulty of a proper interpretation of the NND with respect to localization. The quantities Λ and LL, respectively, are much closer to the original picture of localization drawn by P. W. Anderson and thus one may prefer it in cases where physical intuition is hard to gain. The NND always needs reasonable understanding of the system under examination. (2) While Shima *et al.* focused on the states in the band center of the disordered one-dimensional system, the NND indirectly takes into account the averaged localization property of all states. Assuming that both quantities properly account for localization, it seems that, at least for $(\kappa,\alpha) \in [4,8] \times [2,5]$, the properties of states with $E = 0$ are not dominating enough to show up when all states are included.

As a closing remark we would like to note that the previous discussion points out that the application of the NND as a localization measure is not as straightforward as the other quantities in the particular system we are investigating. Even though it has an appealing property of being basis independent and thus easily employable for studying interacting particles, its interpretation remains complicated. Eventually, this observation prevents us from utilizing it in order to detect localization of multiple particles and we would rather like to argue for an intuitive observable in the section below.

III. LOCALIZATION IN THE PRESENCE OF INTERACTION

In this second part of our discussion on delocalization in the one-dimensional Anderson model, we want to turn to the question how localization is affected by the presence of interaction. This problem basically goes beyond the scope of the quantum physics of H_s originally encountered by Anderson, but—as mentioned in the beginning—the question of the impact of interaction already attracted his attention in the late 1970s. Nevertheless, the problem has remained a challenging topic and experiments with BECs in optical lattices have raised again the focus on it during the past few years.

With Eq. (2) at hand, namely,

$$H_{\mathrm{mp}} = \sum_{i=1}^{L} \epsilon_i c_i^+ c_i + J \sum_{i=1}^{L-1} c_i^+ c_{i+1} + \sum_{i,j=1}^{L} U_{ij} c_i^+ c_j^+ c_i c_j + \mathrm{H.c.}, \tag{19}$$

we introduce an interaction term $U_{ij} c_i^+ c_j^+ c_i c_j$, where for $U_{ij} = U_0 \delta_{ij}$, one encounters the disordered Bose-Hubbard model assuming bosonic commutation relations for the lattice site annihilation and creation operators $c_i^{(+)}$. $U_0 = \mathrm{const}$ describes contact/onsite interaction, i.e., particles interact only when occupying the same site. But as we will carry out in Sec. III B it is convenient to assume the more general case of Eq. (19) to describe experiments with either Rydberg gases[39,40] or dipolar BECs[17] where particles interact even if separated by a large number of lattice sites. In particular, we use an algebraic decaying interaction potential and therefore conceptually bridge from long-range correlation to long-range interaction.

A. Defining localization

Before proceeding, we have to deal with the question on how to treat localization for multiple interacting particles, since localization was originally defined for the single-particle problem. The literature provides several approaches for a suitable definition. For example, one can use the Hausdorff measure[41] as a distance between two states ψ_0 and ψ_t where the latter is the former one evolved in time by the Schrödinger equation $i\hbar\partial_t |\psi\rangle = H_{\mathrm{mp}} |\psi\rangle$. In analogy to Anderson's initiating paper,[1] one can then ask, roughly speaking, for the absence of diffusion in terms of that distance. Another idea is to relate localization to macroscopic observables and associate the notion of localization to vanishing electrical conductivity.[42] Furthermore, one can directly study localization in Fock space as performed, e.g., in Ref. 43. An ansatz independent of the specific form of the Hamiltonian—and thus easily applicable to the interacting problem—is the analysis of spectral statistics, cf. Eq. (7),[32] which is driven by the analogy between random matrices in quantum chaos and the random Hamilton matrices due to disorder. But as extensively discussed in Sec. II B, its strength of being representation independent may come along with some difficulties due to a proper interpretation of the corresponding results. Furthermore, the application of the NND to systems of multiparticles shifts the argument of level repulsion given in Sec. II A to localization in Fock space.

For our purpose, we want to propose a rather intuitive solution inspired by a quantity that seems to be natural under the scope of experiments with cold atoms and which is connected to the particle density. Therefore we try to motivate a projection of the many-particle state to the lattice sites $i = 1, \ldots, L$ and apply a one-particle localization measure afterwards. Of course, the procedure has to coincide with the notion of single-particle localization if we return to a set of Fock states with one particle at a given site.

Since one is able to directly image the density profile of Bose-Einstein condensates in experiment,[12] we consider the question on the probability p_i to find at least one particle at site i. Using the language of second quantization, we define the projection operator

$$\mathcal{P}_i \equiv \frac{c_i}{\sqrt{n_i + \delta_{0n_i}}}, \tag{20}$$

where n_i is the eigenvalue of the number operator $\hat{n}_i \equiv c_i^+ c_i$ counting the number of bosons at site i and the Kronecker delta $\delta_{rr'}$ ensures that $\mathcal{P}_i$ is well defined for $n_i = 0$. Given an

eigenstate $|E\rangle$ of $H_{\rm mp}$, we can answer our question from above by

$$p_i(E) \propto |\langle E|(\mathcal{P}_i^+\mathcal{P}_i)|E\rangle|^2, \tag{21}$$

and the constant of proportionality is obtained by the normalization condition $1 = \sum_{i=1}^{L} p_i$. Therefore we end up with a projection of the multiparticle state $|E\rangle$ onto the site basis $|i\rangle$ by the probability distribution $p_i(E)$. For the single-particle problem, this projection is exactly given by the site basis representation of $|E\rangle$, i.e., $p_i(E) = |\langle i|E\rangle|^2 = \psi_E^2(i)$, whose properties we studied for correlated disorder above. Hence the natural step to perform next is to apply the NSD or the IPR on p_i, where $i = 1,\ldots,L$. But there is an argument excluding the application of the NSD measure: let us suppose that two particles are localized at certain sites i_1 and i_2, i.e., p_i is peaked for $i \in \{i_1,i_2\}$. If $|i_1 - i_2| \sim L$, the NSD will yield values of order one and we would refer to the corresponding $|E\rangle$ as delocalized. Thus we exclusively consider the IPR and our definition of localization turns, roughly speaking, to the association on how many sites are occupied by the interacting particles.

B. Modelling interaction

As announced above, we want to consider long-range correlation inspired by exeriments with dipolar gases. Since no distance Δx between neighboring sites enters the theory, we can think of the limit $L \to \infty$ twofold. It can either refer to approaching an infinitely large system with finite Δx or the continuum limit $\Delta x \to 0$ of a finite total system length $x = L\Delta x$ like in experiments. The following discussion prefers the second picture.

To properly model U_{ij}, let us consider

$$U_{ij} \equiv U(l) \sim l^{-3} \quad \text{for} \quad l \equiv |i-j| \gg 1 \tag{22}$$

according to the dipole-dipole coupling. However, for $l \sim 1$, the interaction has to be renormalized to reach a finite value at $l = 0$, which corresponds to the Bose-Hubbard contact interaction strength U_0. To respect these limits we use the L dependent interaction

$$U_{ij} \equiv U_L^{\pm}(l) = \pm\left(\left[\frac{l}{\lambda_I L}\right]^3 + |U_0|^{-1}\right)^{-1}. \tag{23}$$

We choose the interaction U_{ij} to dependent on the system size L to ensure the constance of the interaction within the picture of the continuum limit described above when L tends to infinity. Note that $\lambda_I > 0$ specifies the range of interaction and the sign $\pm$ determines repulsion and attraction, respectively.

C. Two bosons with dipole-dipole coupling: numerical results

So far our considerations to define localization and the type of interaction were rather general on the total particle number $n = \sum_{i=1}^{L} n_i$ and the system size L, respectively. But for numerical simulations, we need to set up a practically tractable situation; since the dimension of the corresponding Fock space grows exponentially with the total number of particles when assuming constant filling,[44] we investigate the specific case of constant particle number n. Therefore the complexity class of dim $H_{\rm mp}$ shrinks to $\mathcal{O}(L^n)$ and in the specific case of two particles we obtain

$$\dim H_{\rm mp} = \frac{L(L+1)}{2} = \mathcal{O}(L^2), \quad \text{n} = 2. \tag{24}$$

Hence we are able to reach much larger system sizes L in contrast to the situation $L \sim n$ and we are especially interested in the well-established toy model[45–48] of two interacting particles since D. L. Shepelyansky and Y. Imry provide arguments for the invariance of localization with respect to the sign of interaction which we can check numerically. Of course, we do not expect that studying just two interacting particles in a disordered potential will fully account for the effects of finite densities in cold atom experiments, but before turning to full complexity we may gain intuition on the problem by means of this academic example. As we will describe below, there is some phenomenological reasoning that relates delocalization by correlation and interaction.

As in Sec. II B, we apply exact numerical diagonalization to the Hamiltonian $H_{\rm mp}$ and hence we have to specify a suitable basis: We take $\{|n_1 \ldots n_i \ldots n_L\rangle\}$ and Appendix provides details on the explicit form of the Hamilton matrix for arbitrary size $L(L+1)/2$. The inclusion of an interaction term U_{ij} to the problem enlarges our space of system parameters from (κ,α) to $(\kappa,\alpha,\pm u_0,\lambda_I)$, where

$$u_0 \equiv |U_0|/J \tag{25}$$

accounts for the rescaling discussed in the beginning of Sec. II B. We should concentrate on the new degrees of freedom $(\pm u_0,\lambda_I)$ and therefore we fix κ as well as consider uncorrelated disorder $\alpha = 0$ where Anderson localization of all states is a proven fact in one dimension for vanishing interaction. To obtain a measure that characterizes the localization property of the whole system, i.e. for all $|E\rangle$ satisfying $H_{\rm mp}|E\rangle = E|E\rangle$ (parameters κ and α fixed), we convolute IPR(E) extracted from $p_i(E)$ with DOS(E) as performed several times during our numerical studies in Sec. II B, cf. Eq. (11),

$$\overline{\rm IPR}(\pm u_0,\lambda_I) \equiv \int dE\,{\rm IPR}(E){\rm DOS}(E). \tag{26}$$

The corresponding result is shown in Fig. 7. As independently predicted by Shepelyansky and Imry localization seems to be invariant under the transformation $U_{ij} \to -U_{ij}$. Moreover, the range λ_I determines whether the increasing onsite interaction strength u_0 weakly delocalizes or tends to localize the two bosons. This effect sets in when $|U_0| \sim J$, i.e., when the interaction energy becomes comparable to the kinetic contributions in $H_{\rm mp}$.

A plausible argument for the observation that our results yield independence from the sign of the mutual particle interaction relies on a discrete spatial symmetry of the Hubbard Hamiltonian,[49,50] which we apply to Eq. (19). Suppose we transform the spatial wave function $\langle j|E\rangle$ such that all, say, odd site j contributions are inverted and all even ones are left unchanged. The corresponding operator in the basis $\{|j\rangle\}$ reads

$$\mathcal{U} \equiv {\rm diag}(\ldots,-,+,-,+,-,+,\ldots) = \mathcal{U}^+ \tag{27}$$

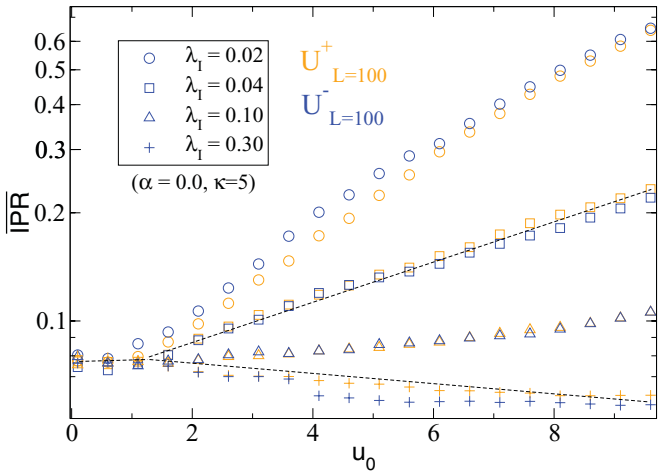

FIG. 7. (Color online) DOS convoluted inverse participation ratio $\overline{\text{IPR}}$ on the basis of the projection, Eq. (21). The quantity was evaluated for several rescaled onsite interaction strengths u_0 and interaction ranges λ_I at fixed $\kappa = 5$. It is remarkable that the result seems to be independent of whether the dipole-dipole coupling is repulsive (orange) or attractive (blue). Furthermore, the plot suggests that λ_I is the crucial parameter to trigger whether increasing interaction strength u_0 delocalizes or localizes the system. Technically, we evaluated systems of size $L = 100$ and averaged over 30 realizations. The black dashed lines sketch the two branches we present in Fig. 8 when additionally considering correlation.

and satisfies $1 = \mathcal{U}^2$, i.e., $\mathcal{U}$ is a unitary transformation. In terms of annihilation/creation operators, one obtains $\mathcal{U} c_j^{(+)} \mathcal{U}^+ = (-)^j c_j^{(+)} = e^{i\pi j} c_j^{(+)}$. Now, the key observation is that

$$\mathcal{U} H_{\text{mp}}(U_0) \mathcal{U}^+ = -H_{\text{mp}}(-U_0) \tag{28}$$

approximately holds when averaging over disorder realizations, cf. Eq. (26), since on average for each set $\{\epsilon_j\}$, there will be another one $\{-\epsilon_j\}$ when $\alpha = 0$. More precisely, if we fix the disorder potential $\{\epsilon_j\}$ the solution $H_{\text{mp}}(-U_0) \left|E'\right\rangle = E' \left|E'\right\rangle$ is related to the solution of $H_{\text{mp}}(U_0) \left|E\right\rangle = E \left|E\right\rangle$ with $\{-\epsilon_j\}$ by the identifications $E' = -E$ and $\left|E'\right\rangle = \mathcal{U} \left|E\right\rangle$, which obviously leaves physical observables/localization measures invariant.

Concerning the qualitative different localization properties of the interacting bosons with respect to the range λ_I, we would like to provide some phenomenological argument that may also draw a unified picture of delocalization by correlation and interaction. Starting from the case of short-range ($\lambda_I \ll 1$), attractive interaction the enhancement of localization may result from the effect of 'lumping': Assume sufficiently strong interaction compared to the kinetic energy $J \lesssim U_0$. Once the particles are nearby, they will be tightly bound in space and the quantum dynamics should be governed by this localized behavior. Due to the approximative invariance of the problem to the interaction's sign the situation surprisingly stays unchanged even for repulsive interacting bosons. But according to Fig. 7, the effect of long-range interaction $\lambda_I = 0.3$ is qualitatively opposite to the short-range case, and we numerically checked that the trend to delocalize with increasing interaction stays up to $\lambda_I = 1$. We would like to note that there is a minor inaccuracy in notion here. Although the algebraic decay of the interaction potential U_{ij} for $|i - j| \sim L$ is always long-ranged compared to, e.g., an exponential decrease, in the following the terms short- and long-range will refer to $\lambda_I \ll 1$ and $\lambda_I \sim 1$, respectively.

One may understand Fig. 7 on the basis of the Fock space Hamilton matrix representation $H_{\text{mp},ff'}$, cf. Appendix, Eq. (A9) and Table I. Since disorder ϵ_i and interaction U_{ij} both contribute to the diagonal elements $H_{\text{mp},ff}$, we may effectively relate the resulting multiparticle Hamiltonian matrix to a corresponding one-dimensional, noninteracting system of size $L(L+1)/2$ with modified disorder $\tilde{\epsilon}_{i'=1\ldots L(L+1)/2}$ and extended dynamics beyond the nearest neighbor hopping.[51] While short-range interaction just contributes to a few diagonal entries of $H_{\text{mp},ff'}$, an increasing interaction range λ_I affects more and more of those matrix elements. Due to the deterministic character of the U_{ij}, i.e. its smooth, algebraic long-range decay, it will effectively correlate the $\tilde{\epsilon}_{i'}$ of the noninteracting analoguous, which we know, to yield delocalization for increasing long-range correlation.

Finally, we want to include long–range correlation $\alpha > 0$ into our toy model of two interacting bosons to directly render the impact of correlation within our localization framework. In Fig. 8, we plot the uncorrelated case from Fig. 7 for two different interaction ranges λ_I as a reference and, therefore, it becomes clear that correlation among the onsite disorder yields delocalization—as we would expect from our previous experience so far, cf. Sec. II B as well as our phenomenological line of reasoning from the preceding paragraph. However, the feature that short-range $\lambda_I = 0.04$ interaction localizes and long-range $\lambda_I = 0.3$ interaction seems to delocalize the two bosons for increasing rescaled interaction strength u_0 is similar to the uncorrelated case.

Again, the result seems to be independent of the sign of interaction. Since we have introduced correlation among the ϵ_i, our argument according to Eq. (28) should not be valid in general. Therefore we suppose the specific disorder model to intrinsically fulfill the necessary assumption from above. Referring to the limiting case $\alpha \to \infty$, we recognize that ϵ_i becomes cosine-like where $\epsilon_i \to -\epsilon_i$ just shifts the onsite potential by a phase value π.

We would like to close our discussion by adding comments on the finite size analysis done as well as comparing our investigations to similar literature, especially Ref. 52, who consider spinless fermions that interact when nearest neighbors to each other—an analogous to the short-range onsite interaction scenario for bosons. Dukesz *et al.* employ the same disorder potential as us and study, among others, the interplay between long-range correlated disorder and interaction for two particles and refer to it as the dilute limit. Their localization detection measure $\langle \text{NPC} \rangle$ is essentially the inverse of our $\overline{\text{IPR}}$, but with the decisive distinction of being applied directly in Fock space—without any projection back to the lattice we advertised in Sec. III A. Therefore we will be restricted to a comparison of qualitative features.

Concerning the left upper panel of Fig. 6 in Dukesz *et al.*, we notice, apart from minor deviation for small interaction strengths denoted by Δ, the trend of enhanced localization, i.e. decreasing $\langle \text{NPC} \rangle$ for increasing interaction strength. A feature that is confirmed by Fig. 7 for sufficiently small interaction

TABLE I. Computation of the matrix elements of H_{mp} in the two-particle basis, Eq. (A10), for general number of sites L.

	Diagonal element $H_{\mathrm{mp},ff}$ contributions								
f:	1	2	...	L	L + 1	L + 2	...	L(L + 1)/2 − 1	L(L + 1)/2
$\epsilon_i c_i^+ c_i$:	$\epsilon_1+\epsilon_1$	$\epsilon_1+\epsilon_2$	...	$\epsilon_1+\epsilon_L$	$\epsilon_2+\epsilon_2$	$\epsilon_2+\epsilon_3$	...	$\epsilon_{L-1}+\epsilon_L$	$\epsilon_L+\epsilon_L$
$U_{i,j} c_i^+ c_j^+ c_i c_j$:	$U_L^{\pm}(0)$	$U_L^{\pm}(1)$	...	$U_L^{\pm}(L-1)$	$U_L^{\pm}(0)$	$U_L^{\pm}(1)$	...	$U_L^{\pm}(1)$	$U_L^{\pm}(0)$
	First off-diagonal elements $H_{\mathrm{mp},ff+1}/J$								
$J c_{i+1}^+ c_i$:	$\sqrt{2}$	1	...	0	$\sqrt{2}$	1	...	0	–
	Remaining off–diagonal elements $H_{\mathrm{mp},ff'}$								
$J c_{i+1}^+ c_i$:	All remaining off-diagonal elements have magnitude J. In the jth off-diagonal ($j \geqslant 1$), there are j								
	Nonzero elements: $H_{\mathrm{mp},ff+j}$ with $f = L - \sum_{r=1}^{j} r = L - j(j+1)/2, \quad \ldots, \quad L - j(j+1)/2 - (j-1).$								

range λ_I: we observe increasing $\overline{\mathrm{IPR}}$. Aside the noninteracting case $u_0 \leftrightarrow \Delta = 0$, this qualtitative trend remains when long-range correlation is involved: according to fixed α, the different $\langle \mathrm{NPC} \rangle$ curves in the lower left panel of Fig. 6 decrease in magnitude. Moreover, each single curve supports enhanced delocalization for increasing correlation parameter $0 \lesssim \alpha \lesssim 4$.

To study effects of finite size it is actually wise to investigate $\overline{\mathrm{IPR}}^{-1}$, since our discussion on Eq. (6) suggests that it provides some notion on the effective number of occupied sites. It is perhaps that stage where one benefits from the proposed projection prescription of Sec. III A again. While $\langle \mathrm{NPC} \rangle$ measures occupation of the eigenstates $|E\rangle$ in Fock space, our $\overline{\mathrm{IPR}}^{-1}$ directly accounts for the projected probability distribution p_i, cf. Eq. (21), on the one-dimensional lattice with L sites. However, in order to establish a finite size analysis, we

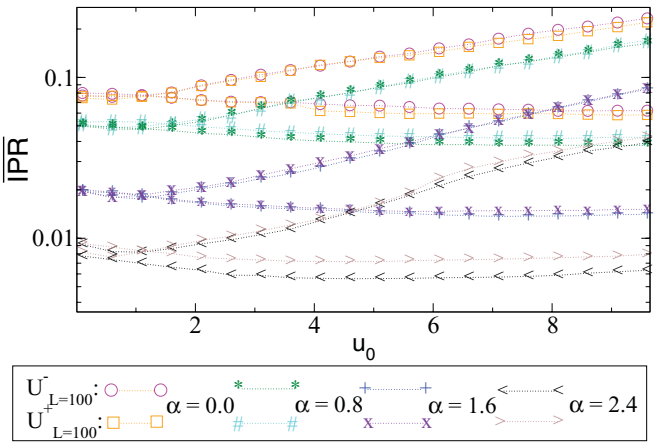

FIG. 8. (Color online) Impact of correlation $\alpha > 0$ on the localization property of two interacting bosons. We picked out two representative branches $\lambda_I = 0.04$ and $\lambda_I = 0.3$ from Fig. 7 to demonstrate that, as expected, correlations tends to delocalize the system. Furthermore, we note that the qualtitative result is again independent of the sign of the interaction and it seems that a feature from $\alpha = 0$ stays untouched, namely, large interaction ranges λ_I weakly delocalize with increasing interaction strength u_0 and for smaller λ_I states localize with respect to increasing u_0. The numerical data were obtained at $\kappa = 5$ from 30 realizations with $L = 100$ sites, which we averaged over.

depicted representative interaction and correlation parameter values $(\alpha,\kappa,u_0,\lambda_I)$ and studied the $\overline{\mathrm{IPR}}$ with increasing system size L in Fig. 9. For uncorrelated $\alpha = 0.0$ and correlated $\alpha = 2.4$ disorders, we chose two different interaction strengths where there is (a) no significant difference in the $\overline{\mathrm{IPR}}$ with respect to Fig. 8, $u_0 = 1$, and (b) where the interaction range λ_I significantly splits the $\overline{\mathrm{IPR}}$, i.e. at $u_0 = 9$, respectively.

In the case of uncorrelated disorder (left and middle left panels of Fig. 9), the averaged number of occupied sites $\tilde{L} = \overline{\mathrm{IPR}}^{-1}$ increases less than linear with linear increasing system size. Thus the extrapolation to the thermodynamic limit suggests localized states as for the non-interacting system. This conclusion is opposite to Dukesz *et al.* who present their results in the lower right panel of Fig. 7 in Ref. 49. It would be interesting to extend there study to larger system sizes beyond $L = 60$. On the other hand, the deviation of the results suggest that a proper projection to the lattice is perhaps crucial in order to investigate localization of multiple particles. However, we would like to point out the increasing deviation of $\tilde{L}$ between short-range and long-range interactions for strong interaction strength u_0, which we like to phrase: 'enhanced delocalization by long-range interaction' and which we suggest to keep in mind for further investigations of interacting particles in disordered media. If we turn to the strongly correlated regime $\alpha > 2$, we definitely observe a qualitative difference in the finite size analysis of $\tilde{L}$. Now the $\overline{\mathrm{IPR}}^{-1}$ seems to grow linearly in L and thus the relative number of occupied sites $\tilde{L}/L$ stays constant for $L \to \infty$ assuming that the observed trend remains for $L > 120$. Hence strong correlation among the disorder potential ϵ_i delocalizes in analogy to the numerical experience from the noninteracting analysis, Sec. II B. But again, in the case of $u_0 = 9$ the curves $\tilde{L}(L)$ increasingly deviate for the scenario of short- and long-range interactions, which verifies our proposal of enhanced delocalization by long-range interaction, and we sketched a potential phenomenological reason by means of a rough correspondence to a noninteracting disordered system above.

In summary, we hope that our data demonstrated that there is a complex interplay between correlation and interaction, which by means of the Hamilton matrix structure may arise

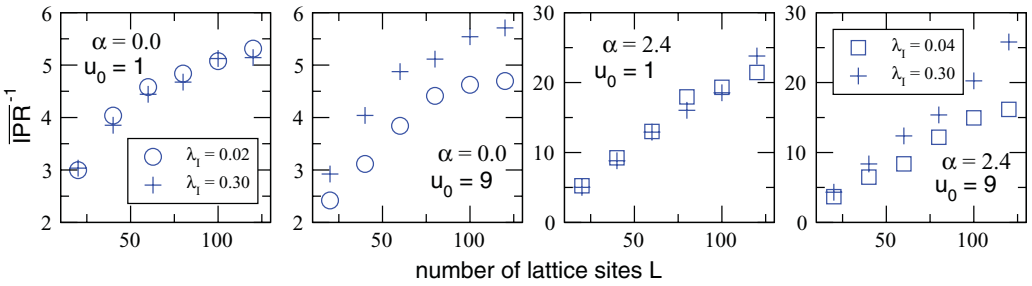

FIG. 9. (Color online) Finite size analysis of the $\overline{\mathrm{IPR}}^{-1}$ for representative model parameter values that specify the correlated disorder by α and the interaction by its strength u_0 and range λ_I. Due to the observed sign symmetry, we restrict to the case of attractive interaction; the color encoding and point shape is kept as in Fig. 7. Instead of plotting the averaged inverse participation ratio $\overline{\mathrm{IPR}}$ itself, it is more appropriate to consider its inverse since it directly relates to the number of occupied sites of the projected probability distribution p_i, cf. Eqs. (6) and (21).

from a similar origin, namely the correlation of the diagonal elements. Furthermore, both effects may compensate each other as seen for $\overline{\mathrm{IPR}}|_{\alpha=0,\lambda_I=0.04}$ and $\overline{\mathrm{IPR}}|_{\alpha=1.6,\lambda_I=0.3}$ at $u_0 \approx 7.5$ in Fig. 8. The numerical study of the interacting bosons supports the independence of localization from the sign of interaction within our picture of multiparticle localization, and we hope that the rather academic treatment of two interacting bosons reveals in experiments with cold gases; at least, in principle, in the limit of sufficiently low densities.[53] Nevertheless, we want to remind that all ideas are based on rather phenomenological reasoning and numerical simulations where we are able to point out qualitative trends only. Therefore our results can just pave the way for a more profound understanding on theoretical grounds.

IV. CONCLUSION AND PERSPECTIVES

To conclude our investigations, we briefly summarize what was achieved within our study of the one-dimensional Anderson model. In the first place, we analyzed two mechanisms that yield delocalization, namely, a correlated disorder potential and mutual interactions between two bosons. By reviewing a known model of correlated disorder from the perspective of exact numerical diagonalization and different well established localization measures, we showed that the process of delocalization is much more complex than observed up to now, namely, there are reasonable arguments to consider $\alpha = 1$ as important for the process of delocalization by correlation. Nevertheless the general trend that increasing correlation yields delocalization was confirmed and localized states approximately vanish for $\alpha \gtrsim 2$. In addition, we were able to numerically establish the full parameter dependence of the model system by means of the nearest neighbor distribution (NND), and therefore we went beyond the analysis that focuses on states in the band center. The results suggest that the system eventually becomes delocalized for sufficient large correlation, independent of the disorder strength κ which is in accordance with Bloch's theorem. Nevertheless, we extensively discussed the usage of the NND and tried to convince that it is far less obvious to utilize it as an localization detection measure.

Therefore we introduced a general idea to define localization for multiparticle states of bosons by means of the phenomenology of experiments with cold quantum gases. The examination of two long-range interacting bosons on a finite, one-dimensional lattice with perfect disorder confirmed the conjecture that the localization property does not dependent on the sign of interaction. We showed that this phenomenon leads back to a discrete symmetry arising when averaging over disorder realizations. Finally, the complex interplay of correlation and interaction was studied numerically, and by means of phenomenological reasoning on the basis of the Hamilton matrix structure, we argued how to relate the impact of interaction to delocalization by correlation known from the noninteracting system.

Although our contribution provides some new insights to the phenomenon of localization, unsolved aspects remain. More precisely, a solid theoretical description of the crossover from localization to delocalization when tuning the nearly perfect disorder to the Bloch-like situation of a highly correlated potential is desired. Moreover, a more profound understanding of the numerically observed effects of interaction on localization is imperative to obtain further insight to delocalization/localization in the presence of many interacting particles.

ACKNOWLEDGMENT

We want to thank Tobias Paul for his collaboration on issues concerning the correlated disorder part of this paper. We are grateful for computational resources provided by the bwGRiD of the federal state Baden-Württemberg, Germany and for support by the Heidelberg Center for Quantum Dynamics as well as the Heidelberg Graduate School of Fundamental Physics, Grant No. GSC 129/1.

APPENDIX: NUMERICAL DETAILS

This Appendix is dedicated to computational details of our work. We especially address the correlated disorder used in the main text and we provide an explicit calculation of the Hamiltonian matrix of two interacting bosons for an arbitrary finite number of lattice sites.

A. Correlated disorder

Here, we provide some properties of the correlated disorder potential ϵ_i and, as a general remark, we mention that all our numerical results were averaged over a certain number

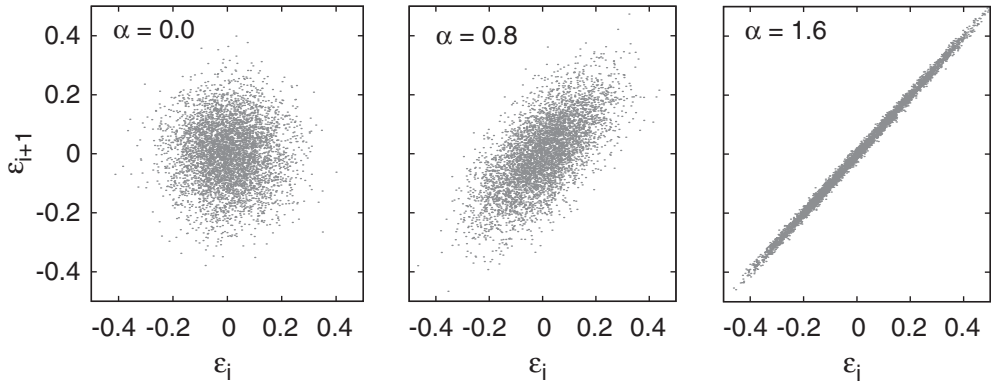

FIG. 10. Illustration of autocorrelation, cf. Eq. (A3), among the onsite disorder ϵ_i, Eq. (3). We evaluated 5000 points $(\epsilon_i,\epsilon_{i+1})$ with $N = 10^5$, cf. Eq. (3). An increasing correlation parameter α deforms the rotationally invariant density of points $(\epsilon_i,\epsilon_{i+1})$ to a linear dependence between ϵ_i and ϵ_{i+1}, which can be quantitatively detected by the linear autocorrelation $C(d)$. Rotational invariance yields $C(1) = 0$ and linear dependence between ϵ_i and ϵ_{i+1} implies $C(1) = \pm 1$. Note, that even in the case $\alpha = 0$, our model disorder is *not* totally homogeneous in $[-0.5,0.5] \times [-0.5,0.5]$.

of disorder realizations. If we exactly follow the prescription Eq. (3) to obtain L values ϵ_i with correlation parameter α, the quantity

$$\delta \equiv \max_i \epsilon_i - \min_i \epsilon_i, \quad i = 1,\ldots,L, \tag{A1}$$

will not be constant in general. To ensure the same disorder strength κ for all disorder realizations and system sizes, we always normalize a given chain of ϵ_i values by

$$\epsilon_i \to \epsilon_i - \min_i \epsilon_i \to \frac{\Delta}{\delta}\epsilon_i \to \epsilon_i - \frac{\Delta}{2} \tag{A2}$$

to have $\epsilon_i \in [-\frac{\Delta}{2},\frac{\Delta}{2}]$. See also Refs. 54 and 55 for a related discussion.

Since we mentioned that $\alpha = 0$ refers to nearly perfect disorder, we provide an intuition on that statement in Fig. 10 where we illustrate increasing correlation by plotting ϵ_i versus ϵ_{i+1} for different α values. For $\alpha = 0$, the point density is approximately rotationally invariant around $(\epsilon_i,\epsilon_{i+1}) = (0,0)$, and for the autocorrelation function,

$$C(d) \equiv \lim_{L\to\infty} \frac{\langle \epsilon_i \epsilon_{i+d}\rangle_L - \langle \epsilon_i\rangle_L \langle \epsilon_{i+d}\rangle_L}{\sigma_{\epsilon_i,L}\sigma_{\epsilon_{i+d},L}}, \tag{A3}$$

where

$$\langle \epsilon_i\rangle_L \equiv \frac{1}{L}\sum_{i=1}^{L}\epsilon_i \quad \text{and} \quad \sigma^2_{\epsilon_i,L} \equiv \langle \epsilon_i^2\rangle_L - \langle \epsilon_i\rangle_L^2, \tag{A4}$$

we find $C(1) \approx 0$ for $\alpha = 0$. Note, that in general, correlation between ϵ_i and ϵ_{i+d} is given by $C(d)$. By means of Eq. (A3), we can state that the disorder is uncorrelated. But as obvious from Fig. 10, the whole plane $(\epsilon_i,\epsilon_{i+1}) \in [-0.5,0.5] \times [-0.5,0.5]$ is not uniformly filled with points $(\epsilon_i,\epsilon_{i+1})$ and therefore an arbitrary on-site potential value ϵ_i can not obviously be followed by any possible ϵ_{i+1}. Thus we refer to the case $\alpha = 0$ as weakly correlated. On increasing correlation we observe that the $(\epsilon_i,\epsilon_{i+1})$ become more and more linearly correlated, i.e., $\epsilon_i \approx \text{const} \times \epsilon_{i+1}$, and thus $C(1) \approx 1$.

Let us finally sketch one feature of the ϵ_i that arises when approximately computing $C(d)$ to demonstrate the long-range character of the correlated disorder. Let

$$\epsilon(x_i) = \int_0^\infty dk\, k^{-\alpha/2}\cos[kx_i + \phi_k], \quad x_i = i\,\Delta x \tag{A5}$$

be the continuous version of Eq. (3) and

$$C(d) \propto \lim_{X\to\infty}\frac{1}{X}\int_0^X dx\epsilon(x)\epsilon(x+d) \tag{A6}$$

that of Eq. (A3). Hence, we obtain

$$C(d) \propto \frac{1}{2}\int_0^\infty dk k^{-\alpha}\cos(kd), \tag{A7}$$

which can be analytically solved for $\alpha \in (0,1)$, and we end up with

$$C(d) \propto d^{\alpha-1} \quad \text{for} \quad 0 < \alpha < 1. \tag{A8}$$

Thus, we have a direct argument at hand why the ϵ_i are long-range correlated. Its spatial autocorrelation decays algebraically, at least in the continuum limit for $\alpha \in (0,1)$, such that increasing α yields a slower decay with distance d. Within this picture, $\alpha = 1$ is also highly correlated and one may argue that delocalization occurs below $\alpha = 2$, which is qualitatively supported by our localization measures although the LL agrees pretty well with other results from the literature, cf. discussion in Sec. II B.

B. Matrix representation of two interacting bosons in the modified/interacting Anderson model

For the numerical results of two interacting particles, we developed a rather general scheme of the matrix representation in Fock space, which allows us to set the numerics for an arbitrary number of sites. Moreover, the matrix is banded with a width $\sim L$, which helps to increase the efficiency of the diagonalization routine. As we were inspired by an experimental setup, we used hard-wall/open boundary conditions, i.e., there is no kinetic hopping element J from site $i = 1$ to site L and vice versa.

TABLE II. Matrix structure of the multiparticle Hamiltonian H_{mp} in the two-particle basis, Eq. (A10), with $L = 6$.

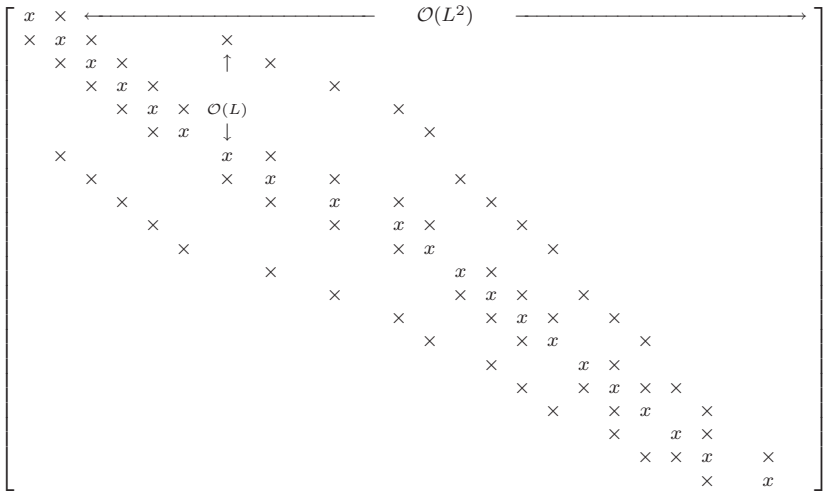

We obtain the matrix structure presented in Table I, if we write the Hamiltonian matrix elements as

$$H_{\mathrm{mp},ff'} \equiv \langle f|H_{\mathrm{mp}}|f'\rangle_F, \tag{A9}$$

where we labeled and ordered the Fock states according to

$$\begin{aligned} |1\rangle_F &= |200\ldots0\rangle, \\ |2\rangle_F &= |110\ldots0\rangle, \\ |3\rangle_F &= |101\ldots0\rangle, \\ &\vdots \\ |L\rangle_F &= |100\ldots1\rangle, \\ |L+1\rangle_F &= |020\ldots0\rangle, \\ &\vdots \\ |L(L+1)/2\rangle_F &= |000\ldots2\rangle, \end{aligned} \tag{A10}$$

with $|n_1 n_2 \ldots n_L\rangle$ indicating the number n_i of bosons at site i. The Hamilton matrix is exemplarily shown for $L = 6$ in Table II. Entries $\times$ denote constant kinetic off-diagonal values and x refers to the diagonal elements that are determined by the correlated disorder terms ϵ_i and the interaction potential U_{ij}.

*c.albrecht@thphys.uni-heidelberg.de

[1] P. W. Anderson, Phys. Rev. **109**, 1492 (1958).

[2] A. Altland and B. Simons, *Condensed matter field theory*, 2nd ed. (Cambridge University Press, Cambridge, UK, 2010), Chap. 2.2.

[3] E. Abrahams, P. W. Anderson, D. C. Licciardello, and T. V. Ramakrishnan, Phys. Rev. Lett. **42**, 673 (1979).

[4] F. Haake, *Quantum Signatures of Chaos* (Springer-Verlag, Berlin, Heidelberg, Germany, 2004).

[5] H. Fürstenberg, Trans. Am. Math. Soc. **108**, 377 (1963).

[6] F. Bloch, Z. Phys. **52**, 555 (1928).

[7] A. M. García-García and E. Cuevas, Phys. Rev. B **79**, 073104 (2009).

[8] F. A. B. F. de Moura and M. L. Lyra, Phys. Rev. Lett. **81**, 3735 (1998).

[9] G. Schubert, A. Weiße, and H. Fehske, Phys. B **359–361**, 801 (2005).

[10] T. Kaya, Eur. Phys. J. B **55**, 49 (2007).

[11] H. Shima, T. Nomura, and T. Nakayama, Phys. Rev. B **70**, 075116 (2004).

[12] J. Billy, V. Josse, Z. Zuo, A. Bernard, B. Hambrecht, P. Lugan, D. Clément, L. Sanchez-Palencia, P. Bouyer, and A. Aspect, Nature (London) **453**, 891 (2008).

[13] L. Sanchez-Palencia and M. Lewenstein, Nat. Phys. **6**, 87 (2010).

[14] P. W. Anderson, Science **201**, 307 (1978).

[15] L. Fleishman and P. W. Anderson, Phys. Rev. B **21**, 2366 (1980).

[16] V. Gurarie, L. Pollet, N. V. Prokof'ev, B. V. Svistunov, and M. Troyer, Phys. Rev. B **80**, 214519 (2009).

[17] A. Griesmaier, J. Werner, S. Hensler, J. Stuhler, and T. Pfau, Phys. Rev. Lett. **94**, 160401 (2005).

[18] J. Stuhler, A. Griesmaier, T. Koch, M. Fattori, T. Pfau, S. Giovanazzi, P. Pedri, and L. Santos, Phys. Rev. Lett. **95**, 150406 (2005).

[19] In our numerics with $L \sim 10^3 - 10^4$, we choose $N_0 = 10^5$ and ensure that our results are not altered for $N > N_0$ by means of finite size analysis, i.e., we do not monitor any qualitative deviation of the data for $N > N_0$.

[20] A. R. Osborne and A. Provenzale, Phys. D **35**, 357 (1988).

[21] E. J. Moore, J. Phys. C **6**, 1551 (1973).

[22]B. Kramer and A. MacKinnon, Rep. Prog. Phys. **56**, 1469 (1993).
[23]T. A. Brody, J. Flores, J. B. French, P. A. Mello, A. Pandey, and S. S. M. Wong, Rev. Mod. Phys. **53**, 385 (1981).
[24]J. M. G. Gómez, R. A. Molina, A. Relaño, and J. Retamosa, Phys. Rev. E **66**, 036209 (2002).
[25]K. B. Efetov, NATO Science Series **221**, 95 (2006).
[26]B. D. Simons and B. L. Altshuler, in *Mesoscopic Quantum Physics: Proceedings of the LXI. Les Houches Summer School* (Elsevier, 1996).
[27]On the basis of coupling two harmonic oscillators, the notion of level repulsion becomes a bit more explicit. In fact, H_s from Eq. (1) just mimics such a system with ground-state energy difference $\Delta\epsilon \equiv |\epsilon_1 - \epsilon_2|$ and ground-state coupling energy J between the two oscillators labeled by $i = 1,2$ in the most simplest case of $L = 2$. By investigating the quantum physics of a single particle in such a setup with $\epsilon_1 = 0$ (w.l.o.g. $\epsilon_2 > 0$), one observes that the energy difference of the system's eigenstates reads $\Delta E \equiv |E_1 - E_2| = 2\sqrt{\Delta\epsilon^2/4 + J^2}$, i.e., in the uncoupled case ($J = 0$), the eigenstates $|E_1 = 0\rangle$ and $|E_2 = \epsilon_2\rangle$ are localized in one of the harmonic oscillators and by tuning the external parameter $\Delta\epsilon \to 0$, their corresponding eigenenergies E_i become degenerate. By means of ΔE this is impossible for $J \neq 0$ where both eigenstates $|E_1\rangle$ and $|E_2\rangle$ are distributed among the two coupled oscillators.
[28]M. Feingold, S. Fishman, D. R. Grempel, and R. E. Prange, Phys. Rev. B **31**, 6852 (1985).
[29]Despite similar in notion, the Lyapunov exponent γ in localization theory has not to be confused with its counterpart in nonlinear dynamics[56] γ where it is often denoted as λ. Here, γ is equivalent to the exponential decay rate of $\psi_E^2(i)$, cf. Eq. (4), for sufficient large systems.
[30]B. I. Shklovskii, B. Shapiro, B. R. Sears, P. Lambrianides, and H. B. Shore, Phys. Rev. B **47**, 11487 (1993).
[31]P. Jacquod, Phys. Rev. Lett. **81**, 1913 (1998).
[32]E. Cuevas, Phys. Rev. Lett. **83**, 140 (1999).
[33]As known from standard text books, e.g., Ref. 4 or F. Dyson's work,[57] the GOE ensemble assumes real valued, symmetric matrices H_{rand} with (a) the joint probability $p(H_{\text{rand}})$ being invariant under orthogonal transformations and (b) one requires the statistical independence of all Hamilton matrix elements.
[34]I. Dumitriu and A. Edelman, J. Math. Phys. **43**, 5830 (2002).
[35]G. Le Car, C. Male, and R. Delannay, Phys. A **383**, 190 (2007).
[36]P. Jacquod and D. L. Shepelyansky, Phys. Rev. Lett. **79**, 1837 (1997).
[37]S. N. Evangelou, J. Stat. Phys. **69**, 361 (1992).
[38]While we directly rely on Eq. (3) to produce correlated disorder see also Appendix, Ref.11 performs some sort of Fourier filtering method to obtain long-range correlated ϵ_i values.
[39]W. Li, P. J. Tanner, and T. F. Gallagher, Phys. Rev. Lett. **94**, 173001 (2005).
[40]K. Singer, M. Reetz-Lamour, T. Amthor, L. G. Marcassa, and M. Weidemüller, Phys. Rev. Lett. **93**, 163001 (2004).
[41]M. Aizenman and S. Warzel, Commun. Math. Phys. **290**, 903 (2009).
[42]D. M. Basko, I. L. Aleiner, and B. L. Altshuler, Ann. Phys. **321**, 1126 (2006).
[43]R. Berkovits and Y. Avishai, Phys. Rev. Lett. **80**, 568 (1998).
[44]Constant filling means $n \sim L$ and together with $\dim H_{\text{mp}} = (n + L - 1)!/(n!(L - 1)!)$ from elementary combinatorics and Stirling's approximation $\ln x! \sim x \ln x - x$, we obtain $\dim H_{\text{mp}} \sim a^L$ for $L \gg 1$ and a of order 1.
[45]D. L. Shepelyansky, Phys. Rev. Lett. **73**, 2607 (1994).
[46]Y. Imry, Europhys. Lett. **30**, 405 (1995).
[47]K. Frahm, A. Müller-Groeling, J.-L. Pichard, and D. Weinmann, Europhys. Lett. **31**, 169 (1995).
[48]R. A. Römer and M. Schreiber, Phys. Rev. Lett. **78**, 515 (1997).
[49]K. Sakmann, A. I. Streltsov, O. E. Alon, and L. S. Cederbaum, Phys. Rev. A **82**, 013620 (2010).
[50]U. Schneider *et al.*, e-print arXiv:1005.3545v1 (unpublished).
[51]We would like to remind that Anderson's initiating paper[1] did not restrict to the case of nearest neighbor hopping. That was also the reason why we mentioned to deal with a certain subclass of Hamiltonians, Eq. (1), in Sec. I.
[52]F. Dukesz, M. Zilbergerts, and L. F. Santos, New J. Phys. **11**, 043026 (2009).
[53]For this purpose, it is obviously necessary to produce correlated long-range disorder with algebraic power spectrum, which could be a challenging task for experiments. Via Feshbach resonances,[58] it is possible to tune the interaction strength u_0, but the variation of the range λ_I is perhaps difficult to establish.
[54]J. W. Kantelhardt, S. Russ, A. Bunde, S. Havlin, and I. Webman, Phys. Rev. Lett. **84**, 198 (2000).
[55]F. A. B. F. de Moura and M. L. Lyra, Phys. Rev. Lett. **84**, 199 (2000).
[56]S. Strogatz, *Nonlinear dynamics and chaos: With applications in physics, biology, chemistry and engineering* (Perseus Books Publishing, Massachusetts, USA, 1994), Chap. 10.5.
[57]F. J. Dyson, J. Math. Phys. **3**, 140 (1962).
[58]W. Ketterle and W. Zwierlein, in *Proceedings of the International School of Physics "Enrico Fermi,"* (2008).